PERGAMON

Chemical Engineering Science 58 (2003) 3935–3945

Chemical Engineering Science

www.elsevier.com/locate/ces

Effective interfacial area in agitated liquid–liquid continuous reactors

Paulo A. Quadros, Cristina M. S. G. Baptista*

Gepsi-PSE Group, Department of Chemical Engineering, University of Coimbra, Pólo II, Pinhal de Marrocos, 3030-290 Coimbra, Portugal

Received 17 December 2002; received in revised form 2 June 2003; accepted 22 June 2003

Abstract

A chemical method has been used to quantify the effective interfacial area in a baffled continuous stirred liquid–liquid reactor. Two and four straight paddle impellers were used in the experimental runs, at 34°C, with hold-up fractions of dispersed organic phase between 0.061 and 0.166 and stirring speed ranging from 360 to 1500 rpm. Influence of the residence time on the formation of the interfacial area generated in this system was not registered; however, differences were reported between continuous and batch mode operations.

The interfacial area was correlated to hold-up fraction and Weber number by a new empirical model proposed in this work. This model allows to use only one equation to calculate the interfacial area in this continuous stirred reactor in the wide range of operating conditions tested ($490 < We < 9600$), which include different flow regimes. This is a relevant contribution as previous studies in this field only contemplate turbulent flow. In the transitional regime the mean drop size diameter decreases abruptly with Weber number, but this pattern changes in the higher range of Weber where the dispersed drops become smaller very smoothly. This pattern does not depend on the agitator used or hold-up fraction. The mean drop size diameter is smaller for the four paddle impeller and increases with hold-up fraction. The model developed may be applicable to dispersions in aromatic nitration reactors, improving its operation and design.
© 2003 Elsevier Ltd. All rights reserved.

Keywords: Multiphase reactors; Interfacial area; Liquid–liquid; Drop size; Model; Dispersion

1. Introduction

Numerous industrial processes involve two liquid reacting phases and are processed in continuous flow reactors. A better understanding of one of these processes, the nitration of benzene carried out under operating conditions used in industrial practice, is the subject of our research project. One of the first steps to correctly understand the mechanisms involved in these processes is to know the effective interfacial area available in the reacting system. Several authors presented physical and chemical methods to determine the interfacial area in different liquid–liquid systems. The former methods make use of only the physical properties of the system, while the last ones measure the physical process of mass transfer and an accompanying chemical reaction (Cieszkowski & Dylag, 1994). The physical methods make use of optical, photographic or electrolytic resistance measurement techniques (Vermeulen, Williams, & Langlois, 1955; Eckert, McLaughlin, & Rushton, 1985) and, according to Westerterp, Van Dierendonck, and De Kraa (1963), these methods determine local values of the interfacial area, which cannot be representative of the entire system. Furthermore, these techniques may require the introduction of measuring equipment in the reactors that interfere with the normal flow pattern and may bias the final result. Westerterp et al. (1963) were the first to develop the chemical method to evaluate the interfacial area in a gas–liquid system. This technique consists in following the extraction of a reactant from one phase to the other, which is accompanied by an irreversible and fast pseudo-first-order reaction, enabling to quantify the interfacial area through the mass transfer between phases. Nanda and Sharma (1966) adapted this method to liquid–liquid systems and since then several authors (Vázquez, Cancela, Riverol, Alvarez, & Navaza, 2000 and van-Woezik & Westerterp, 2000) used this procedure to determine interfacial areas in gas–liquid and liquid–liquid systems. The major advantage of this approach is that it allows determining the global values of the interfacial area in the heterogeneous systems, which are dependent on design and operating conditions, without interfering with

* Corresponding author. Tel.: +351-239-798-738; fax: +351-239-798-703.
E-mail address: cristina@eq.uc.pt (C. M. S. G. Baptista).

0009-2509/$ - see front matter © 2003 Elsevier Ltd. All rights reserved.
doi:10.1016/S0009-2509(03)00302-6

the flow pattern and this can hardly be achieved with the physical methods. Nevertheless, the chemical method cannot give information on drop size distribution across the reactor.

In a heterogeneous liquid–liquid reacting system, the effective interfacial area is an important variable for design, its accurate evaluation being crucial to a good understanding and quantification of mass transfer and chemical reaction phenomena occurring during a heterogeneous liquid reaction. It is well known that interfacial area depends on a very large number of parameters, including the mixing conditions, and numerous studies and correlations relating the physical, chemical and mechanical characteristics of these systems have been published (see Fernandes & Sharma, 1967; Coulaloglou & Tavlarides, 1976). However, these studies often contradict each other being not conclusive; therefore, it is not always possible to make use of the results in other systems.

The interfacial area can be calculated by Eq. (1) where ε is the volumetric fraction of the dispersed phase (hold-up fraction) and d_{32} the Sauter mean drop diameter of the dispersed phase.

$$a = \frac{6\varepsilon}{d_{32}}. \tag{1}$$

The size of the drops of the dispersed phase can be obtained by the semi-empirical equation

$$\frac{d_{32}}{D} = A(1 + B\varepsilon)We^{-0.6}, \tag{2}$$

where D is the impeller diameter, We is the dimensionless Weber number and A and B are parameters dependent on the reacting system. Different authors use different exponents for the Weber number (Fernandes & Sharma, 1967; Godfrey, Obi, & Reeve, 1989). These disagreements are related to the fact that all the phenomena associated with interfacial area formation are not yet fully understood, namely the break-up and coalescence effects (Ribeiro, Regueiras, Guimarães, Madureira, & Cruz-Pinto, 1997; Balmelli, Steiner, & Hartland, 2000; Lasheras, Eastwood, Martínez-Bazán, & Montañés, 2002). The flow regime in the vessel is also relevant. For low stirring speed, Eq. (2) cannot correctly predict the mean drop diameter and the exponent on the Weber number depends on the range of mixing conditions used in experiments (Fernandes & Sharma, 1967). Therefore, this equation should only be used in a stirring range where the turbulent flow regime is completely developed, one of its main limitations being the inability to correctly predict the interfacial area generated at lower stirring speeds where the transitional flow regime between laminar and turbulent flow occurs. However, Eq. (2) is often used, leading to satisfactory results in the high stirring speed range (van-Woezik & Westerterp, 2000).

Based on chemical principles, Starks (1999) developed a theoretical equation for interfacial area formation in laminar flow. This equation does not have adjustable parameters and was obtained for an unbaffled reactor. This limits its application to other studies and in industrial practice since most of these reactors are baffled, in order to promote turbulence even at low stirring ranges. Starks (1999) used the experimental results from Vermeulen et al. (1955) to validate his equation and obtained average errors of approximately 23%, which can be considered remarkably good.

Having in mind a generalized and systematic analysis of the interfacial area formation in agitated systems, Eckert et al. (1985) undertook a study that shows its dependence on seven parameters. These can be grouped in three different categories: system composition, fluid properties and mechanical conditions. Eckert et al. (1985) first obtained an empirical equation with 17 terms, which were later reduced to eight to simplify its application. In spite of this effort, Eckert et al. (1985) did not achieve better results than Eq. (2). Their major contribution was the evaluation of property interactions and providing an equation to be used in scale-up and to predict interfacial area in new systems, which is not achievable with other equations. am Ende, Eckert, and Albright (1995) studied the interfacial area of sulphuric acid and hydrocarbons dispersions using a stirred reactor and a constant cross-sectional area reactor, and concluded that interfacial area is dependent on hold-up fraction of the dispersed phase, on acid composition, on agitation speed and temperature and added that interfacial area reaches a maximum which depends on the volume of the continuous phase. Furthermore, these authors used image analysis and registered a bimodal distribution of droplets diameters that has been confirmed at high phase ratio by Desnoyer, Masbernat, and Gourdon (2003). This recent work also reports that, for the high phase ratio liquid–liquid dispersions studied, the exponent on Weber number in Eq. (2) is a decreasing function of the phase ratio. The influence of vessel size upon drop size formation, which is not considered in Eq. (2), has been registered by Baldyga, Bourne, Pacek, Amanullah, and Nienow (2001) when studying the effects of agitation and scale-up on drop size dispersions.

The studies undertaken show that the phenomena involved in this process are so complex that a complete and rigorous theoretical study is nearly impossible, since it is very difficult to extrapolate results and conclusions in between different systems and, as Podgórska and Baldyga (2001) observed, there are different scale-up criteria. Therefore, when the interfacial area data for the system and reactor in use are not available, it is advisable to conduct experiments in order to estimate it.

The main purpose of the work reported here is to study the influence of some parameters upon interfacial area formation in a continuous stirred tank reactor, part of a pilot plant, to be used for kinetic studies of benzene nitration with mixed acid, which is enhanced by mass transfer.

2. Chemical method

2.1. Theory

In order to determine the interfacial area of a particular liquid–liquid system, this study will use the chemical method developed by Westerterp et al. (1963) for gas–liquid systems and later adapted for liquid–liquid mixtures by Nanda and Sharma (1966). The interfacial area for the system will be obtained by quantifying the amount of reactant A from the organic dispersed phase that is extracted to the aqueous phase, where it reacts very fast with reactant B. This extraction followed by reaction from now on will be referred to as extraction. In a steady-state regime, a mass balance to reactant A in the organic phase of a continuous stirred reactor assumes the following form:

$$0 = F_A^{\text{in}} - F_A^{\text{out}} - a J_A V, \tag{3}$$

where a is the effective interfacial area of the reactor, F_A^{in} and F_A^{out} are the inlet and outlet molar flow rates of reactant A in the organic phase. The molar flux of reactant A between phases is represented by J_A and V is the reactor volume. In Eq. (3), the molar flux of A, J_A, cannot be obtained straight from the data collected during experiments with the continuous stirred reactor, as the effective interfacial area of the reactor is also unknown. According to Zaldivar, Molga, Alós, Hernandez, and Westerterp (1996), the molar flux of A into the aqueous phase is dependent on the physical–chemical properties of the reacting mixture and not on the hydrodynamics of the system and can be calculated by Eq. (4):

$$J_A = C_{A,\text{aq}}^{i} \sqrt{kD_A} = m_A C_{A,\text{org}} \sqrt{kD_A}. \tag{4}$$

Therefore, the term $m_A \sqrt{kD_A}$ can be obtained in a different reactor, for instance a cell reactor with known interfacial area. Once this term is known, it is possible to determine the effective interfacial area in any kind of equipment (e.g. stirred reactor, plug flow reactor or extraction column) as long as the requirements of the chemical method remain valid. In this case, combining Eqs. (3) and (4) enables obtaining the effective interfacial area as a function of data known or determined in experiments:

$$a = \frac{F_A^{\text{in}} - F_A^{\text{out}}}{m_A \sqrt{kD_A} C_{A,\text{org}}^{\text{out}} V}. \tag{5}$$

2.2. Selecting the adequate reacting system

Not every reactant or reacting system fulfils the requirements of the chemical method. As Zaldivar et al. (1996) and van-Woezik and Westerterp (2000) stated, Eq. (4) can only be used if the following conditions are fulfilled:

- The reaction is so fast that A does not reach the bulk of the aqueous phase reacting with B at the interface. Nevertheless, the solubility of A in the aqueous phase must be very low, so mass transfer limitations in the organic phase can be neglected.
- The concentration of B in the aqueous phase (bulk and interface) can be presumed constant during the process and therefore pseudo-first-order reaction is assumed.

For these reasons, the composition of the organic and aqueous phases has to be carefully chosen. Sankholkar and Sharma (1973) refer to several systems that can be used. They studied the extraction followed by reaction of olefins into aqueous solution of sulphuric acid and concluded that, at 30°C, the extraction into sulphuric acid solutions (72–77wt%) of diisobutylene (2,4,4-trimethyl-2-pentene, here referred to as DIB-2) diluted in toluene or chlorobenzene can be considered an adequate chemical reacting system. Moreover, Sankholkar and Sharma (1973) mentioned that the diisobutylene solubility in water is extremely low and that this olefin can be diluted in any appropriate organic liquid that does not react with sulphuric acid without introducing any resistance into the organic phase, therefore, fulfilling the requirements of the chemical method. The similarity of the mixtures physical–chemical properties to the properties of the reagents used in the kinetic process under study is one of the criteria used on selection. This similarity is very important because it will enable to ensure that the aggregation and coalescence effects, which are difficult to quantify, will show identical behaviour to the process system under study. To study the toluene nitration, Zaldivar et al. (1996) used a reacting system similar to the one used by Sankholkar and Sharma (1973), with some changes. Having in mind that information from the chemical method will be used on the nitration of benzene with sulphuric acid as a catalyst, we selected a reacting system identical to the one used by Zaldivar et al. (1996) introducing some modifications in accordance with our system. We used an isomer mixture of 2,4,4-trimethyl-1-pentene (DIB-1) and 2,4,4-trimethyl-2-pentene (DIB-2) in the proportion 3:1 supplied by Fluka, diluted in benzene, with the total molar DIB concentration of 7%, and performed the tests at 34°C with sulphuric acid at 77.5% (wt). According to Schiefferle, Hanson, and Albright (1976), at 34°C, the benzene solubility in this sulphuric acid solution is similar to that exhibited by the compounds suggested by Sankholkar and Sharma (1973), being of the same order of magnitude as the solubility of toluene and chlorobenzene. In order to follow the extraction of DIB-1 and DIB-2 into the aqueous phase, where they react with sulphuric acid (Zaldivar et al., 1996), the composition of the organic phase was analysed in a gas chromatograph 9001 Tremetrics, provided with a silica gel DB-1 J & W column. Gehlawat and Sharma (1968) and Carey (1992) refer to this reaction mechanism that involves two steps: the sulphuric acid addition to DIB-1 and DIB-2 producing both the 2,4,4-trimethyl-penthyl-2-hydrogen sulphate followed

by its hydrolysis into 2,4,4-trimethyl-2-pentanol with regeneration of the sulphuric acid. Once it is known that these reactions are very fast it is considered that they occur across the interface. The adequacy of this reaction system and the fulfilment of the chemical method requirements was confirmed by the GC analysis that show, in both stirred cell experiments and in the pilot plant reactor, a peak corresponding to 2,4,4-trimethyl-2-pentanol. This is a product of DIB reactions which is partially soluble in the organic phase and would not be detected if the reaction was a slow process compared to the rate determining extraction step. This reacting system has been used in the experiments in the batch stirred cell with known interfacial area and in the pilot plant.

2.3. Determination of the term $m_A\sqrt{kD_A}$

A batch-jacketed stirred cell system was used to determine the term $m_A\sqrt{kD_A}$. It consists of an unbaffled reactor built with two concentric borosilicate glass tubes fixed between two PTFE plates. Its dimensions are summarized in Table 1. This stirred cell has a known interfacial area of $A_{sc} = 67.53$ cm^2 and a two straight paddle teflon agitator. Only the heavy aqueous phase was stirred, at low agitation speed, avoiding vortex or interference with the interfacial area of the cell, but promoting the renoval of the interface between the two liquid phases. A thermostatic bath was used to keep the temperature in the mixing cell constant at 34°C, by circulating water through the reactor's jacket.

Each experiment was carried out for 53 h using 600 ml of acid solution and 80 ml of organic phase as these volumes disable vortex formation. The decrease of DIB in the organic phase was followed by withdrawing small amounts of the upper phase that were then analysed by GC. These withdrawals were spaced in time for at least 7 h and the five samples collected per experiment did not exceed a total volume of 4 ml, which is less than 5% of the total volume of the organic phase, allowing one to assume that the volume of this phase is kept constant along the duration run.

The mass balance to DIB in the organic phase in the batch-stirred cell leads to Eq. (6):

$$V_{\text{org}}\frac{dC_{\text{DIB,org}}}{dt} = -A_{sc}\,C_{\text{DIB,org}}\,m_{\text{DIB}}\sqrt{kD_{\text{DIB}}}. \tag{6}$$

Normalizing DIB concentration and integrating one obtains Eq. (7).

$$\ln\frac{C_{\text{DIB, org}}}{C^0_{B,\text{ org}}} = \ln\frac{C^0_{\text{DIB,org}}}{C^0_{B,\text{org}}} - \frac{A_{sc}}{V_{\text{org}}}\,m_{\text{DIB}}\sqrt{kD_{\text{DIB}}}\,.t. \tag{7}$$

The concentration's of DIB-1 and DIB-2 were measured and the data plotted in Fig. 1 show that the extraction of these olefins is a slow process. Since the concentration of DIB-1 is higher and easier to measure than DIB-2, we decided to calculate the specific extraction term based only on DIB-1 extraction to the aqueous phase.

Table 1
Dimensions of the stirred cell

Diameter (cm)	9.35
Height (cm)	14.93
Volume (cm^3)	1025
Impeller diameter (cm)	3.10
Agitator diameter (cm)	1.20

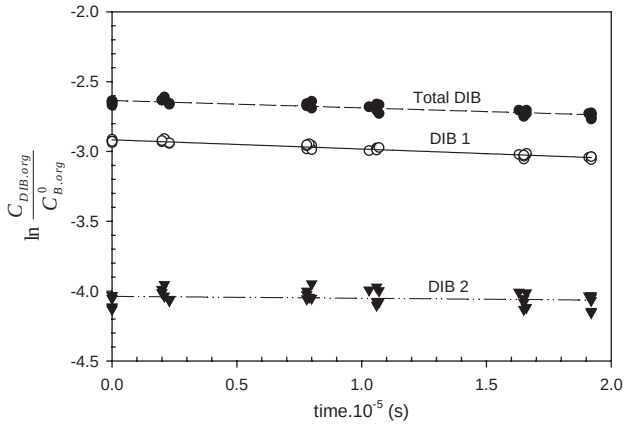

Fig. 1. Individual and total concentrations of diisobutylenes versus time in the stirred cell experiments.

Table 2
Specific extraction term obtained at different stirring speeds

Run	N (rpm)	$m_{\text{DIB}}\sqrt{kD_{\text{DIB}}} \times 10^9$ (m s^{-1})
A	140	7.81
B	140	8.42
C	170	7.82
D	170	7.41
E	200	7.49
F	230	8.23

In order to confirm that $m_{\text{DIB}}\sqrt{kD_{\text{DIB}}}$ is not dependent on the hydrodynamics of the system and depends only on the physical–chemical properties of the reacting system, different stirring speeds were used to corroborate this assumption. Table 2 summarizes the values of the extraction term of DIB obtained at different stirring speeds.

These results confirm that, for the conditions tested and reacting system used, the specific rate of extraction does not depend on the hydrodynamic factors and that there are no limitations to mass transfer in the organic phase. Moreover, since their average relative error is 3.9%, which is very good for experimental data and better than in other authors for similar systems, see Zaldivar et al., 1996, in further calculations the average value of this term will be used i.e., $m_{\text{DIB}}\sqrt{kD_{\text{DIB}}} = 7.86 \pm 0.56 \times 10^{-9}$ m s^{-1}. These results also confirm the adequacy of the reacting system used in this

work to measure and determine the interfacial area by the chemical method.

3. Interfacial area determinations in the pilot plant

3.1. Description of the experimental apparatus

The continuous jacketed reactor was built with two concentric borosilicate glass tubes fixed between two PTFE plates, with an approximate capacity of 1 l. The reactor is equipped with a temperature sensor, four tantalum baffles and with a two or a four straight-paddle-type agitator, which is driven by a pneumatic Atlas Copco driver. The stirring speed was measured by a digital tachometer and registered by the computer. The reactants are stored in pressurized vessels and were fed separately by Q1SAN model FMI metering pumps, which were regulated to the required flow rate. During operation, the reactor was completely full, as the reactants were fed at the bottom and withdrawn from the top. A thermostatic bath that feeds the reactor's jacket was used to control and keep the temperature constant. Every process variable, temperature, flow rate, residence time, stirring speed and reactant level in pressurized vessels was monitored by computer. A concise illustration of our pilot plant is represented in Fig. 2 and the main dimensions are summarized in Table 3.

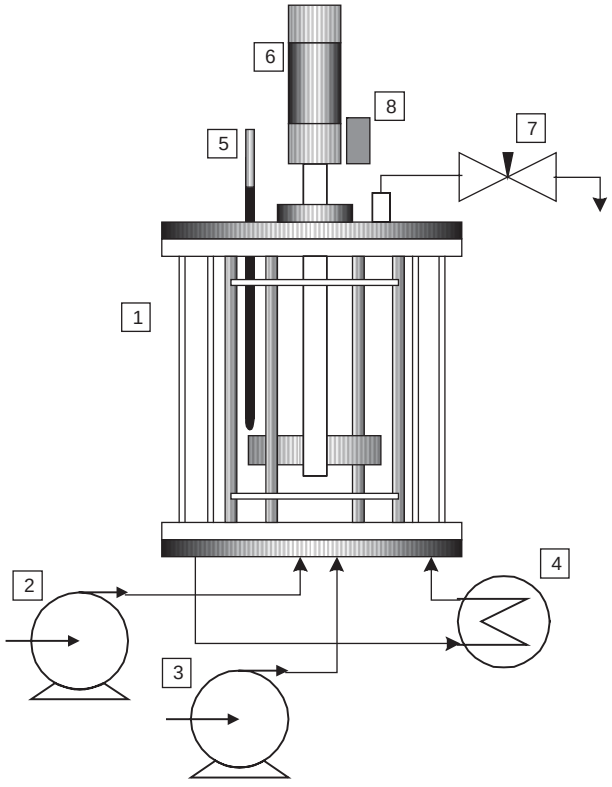

Fig. 2. Schematic representation of the pilot plant. 1, continuous stirred reactor; 2, benzene and DIB-1 + DIB-2 feed pump; 3, sulphuric acid feed pump; 4, thermostatic bath; 5, temperature sensor; 6, pneumatic driver; 7, sampling valve; 8, tachometer.

Table 3
Dimensions of the continuous stirred reactor

Diameter (mm)	95.0
Height (mm)	151.0
Baffles diameter (mm)	10.5
Number of baffles	4
Volume (dm^3)	1.060
Distance of the agitator from the bottom (mm)	50.0
Two straight paddle agitator	
Impeller diameter (mm)	54.0
Paddle height (mm)	10.7
Four straight paddle agitator	
Impeller diameter (mm)	50.8
Paddle height (mm)	10.0

3.2. Experimental procedure

The runs were started by turning on the feeding metering pumps, the pneumatic driver and the thermostatic bath, and carried on till constant profiles of the monitored parameters were attained. The flow rates were adjusted through the metering pumps so that the acid phase has been the continuous phase within a selected range of hold-up fraction and residence time is reported in Tables 4 and 5. Once steady state was attained, a sample of the mixture was collected very close to the reactor outlet by a needle valve and the stirring speed was changed to a new set point. It would take 3–5 residence times to reach another stationary state and collect another reacting sample. The samples collected were allowed to separate phases, which was a very fast process. The organic phase was prepared for GC analysis following the procedure used in the stirred cell experiments. Using in these runs the same reactants as in the stirred cell experiments ensured the reproducibility of results.

4. Results and discussion

The aim of this study is the quantification of the interfacial area in a continuous stirred reactor. However, to confirm the information in Coulaloglou and Tavlarides (1976) and Godfrey et al. (1989) that in lower stirring range continuous and batch operation lead to different drop size diameters, the stirred reactor has been operated continuously and batch wise. The same hold-up fraction range has been used and the formation of a completely dispersed mixture in the batch mode operation occurred only for a stirring speed greater than 1100 rpm, while in continuous operation the dispersion was detected even for stirring speeds that were lower than 400 rpm. In batch operation, when the stirring speed was settled below 800 rpm, there were clearly two immiscible zones and the reactor effective interfacial area tends to the cross-section area of the reactor, as experienced in the stirred cell runs performed to evaluate the term $m_{\mathrm{DIB}}\sqrt{kD_{\mathrm{DIB}}}$. This

Table 4
Experimental conditions used in runs with the two-paddle agitator

Run	Number of steady states	ε	N (rpm)	τ (min)	We
1	9	0.061	417–1455	3.0	783–9559
2	9	0.099	390–1458	3.0	687–9594
3	7	0.102	378–1090	3.0	646–5357
4	8	0.118	371–1331	6.0	622–7993
5	9	0.166	459–1431	2.7	950–9241

Table 5
Experimental conditions used in runs with the four-paddle agitator

Run	Number of steady states	ε	N (rpm)	τ (min)	We
6	10	0.070	367–1464	3.3	507–8049
7	10	0.096	370–1493	3.4	513–8376
8	10	0.102	361–1489	3.8	491–8324
9	9	0.108	363–1287	2.8	494–6227
10	9	0.164	370–1445	2.7	515–7848

confirms previous records of different interfacial area formation according to the operation mode of the reactor and stresses the importance of the hydrodynamic characteristics of the flow in the reactor.

During the continuous operation of the stirred reactor, two impellers were tested (see Table 3), but their location was not changed. For each impeller, the influence of the hold-up fraction of the dispersed organic phase has been examined within the range $0.061 \leqslant \varepsilon \leqslant 0.166$. As previously described, during the runs the stirring speed has been increased, the minimum value tested being 361 and the maximum 1493 rpm. A total number of 90 steady states have been attained and the working conditions used are summarized in Tables 4 and 5 for the two and four paddle agitators, respectively.

All these experiments were conducted under isothermal conditions at 34°C ± 0.5°C, with sulphuric acid at 77.5% (wt) and an aqueous phase density of 1686.8 kg m^{-3}. The interfacial tension was measured with a KSV Sigma 70 ring tensiometer, the average value at 34°C is 16.35 mN m^{-1}.

In Fig. 3, the mean drop size diameter is represented as a function of the Weber number for the five runs conducted in continuous mode with the four-paddle impeller. In the lower We range the decrease in d_{32} is abrupt but this pattern changes in the higher range of We where the dispersed drops become smaller very smoothly. The same pattern for the drop size was obtained in the experiments with the two paddle impeller and with different hold-up fractions. This evidence supports that there are two distinct We operation ranges, i.e., a lower region of We corresponding to a transitional flow regime and an upper zone of We with turbulent flow.

Notice that no residence time influence was detected in the drop size formation in the runs plotted in Fig. 3 or in the runs conducted with the two-paddle impeller. In the range of residence time studied (2.7–6.0 min), the size of the drops formed is independent of residence time, as already reported by Godfrey et al. (1989) when testing continuous operation with residence times between 2 and 4 min.

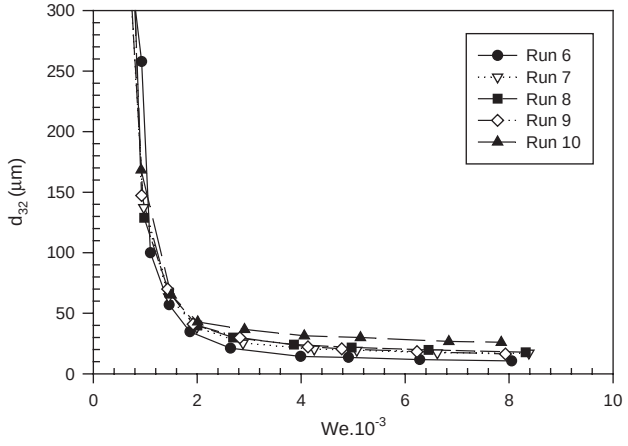

Fig. 3. Influence of the Weber number on the drop size diameter for the four paddle impeller.

Turbulent flow regime, which corresponds to small drop sizes, has been studied by several authors and, as referred to in the introduction, the d_{32} is correlated to Weber number and the hold-up fraction by Eq. (2). In literature, the limit for the turbulent flow regime in agitated liquid–liquid systems is not completely settled, but the data plotted in Fig. 3 allow us to assume that, for the acid-continuous system tested, a turbulent flow regime is established for Weber numbers higher than 1900. Within the experimental accuracy, our results in this range confirm a dependency of d_{32} on $We^{-0,6}$. In Fig. 4, the drop size diameter and Eqs. (8) and (9) are represented as a function of Weber number for runs 4 and 9, which

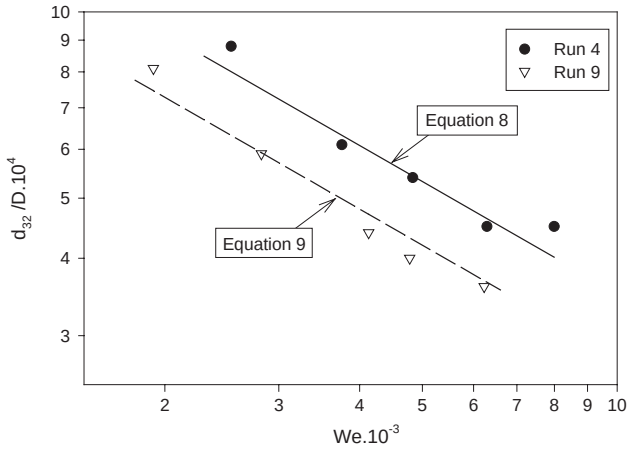

Fig. 4. Influence of Weber number on the drop size diameter for the two and four paddle impeller—Eqs. (8) and (9).

correspond to two and four paddle impellers, respectively. In every run it was observed that, for the same Weber number and similar hold-up fraction, the four-paddle impeller always produces drops of smaller size than the two-paddle impeller. Correlating the Sauter diameter data with hold-up fraction and Weber number using Eq. (2), a good agreement was achieved and Eqs. (8) and (9) were obtained for the reacting system under study. The number of paddles in impeller and their size has influence on drop size diameter as the constants in Eqs. (8) and (9) reveal, nevertheless these constants are of the same magnitude.

Two-paddle impeller:

$$\frac{d_{32}}{D} = 0.0336(1 + 13.76\varepsilon)\, We^{-0,6} \quad We > 1900. \tag{8}$$

Four-paddle impeller:

$$\frac{d_{32}}{D} = 0.0286(1 + 13.24\varepsilon)\, We^{-0.6} \quad We > 1900. \tag{9}$$

For most of the runs, the relative error obtained with these equations is less than 12%; however, in some cases the error was bigger. If the exponent on *We* is left as an adjustable parameter this error can decrease, therefore it is our understanding that in some runs, for Weber numbers close to 1900, the system is in the transitional regime and not in a fully established turbulent flow. In 1967, Fernandes and Sharma related the drops' diameter to the stirring speed with an exponent −1 for high stirring speed and observed that when the lower stirring speed range is included this power changed to −1.5. This corroborates our statement that Eq. (2) may not be the most adequate to correlate drop size diameters, particularly when turbulent flow regime is not completely developed.

As it has been mentioned, it is not easy to establish the lower limit for the range of Weber number, where Eqs. (8) and (9) fit the experimental data. Moreover, when modelling chemical processes, it is important to use equations

Table 6
Constants for the calculation of the effective interfacial area—Eq. (10)

Impeller	Number of data used	C_1	C_2	C_3	Correlation coefficient
Two paddle	42	0.22	−1.40	2.41	0.9858
Four paddle	48	0.19	−1.48	2.55	0.9929

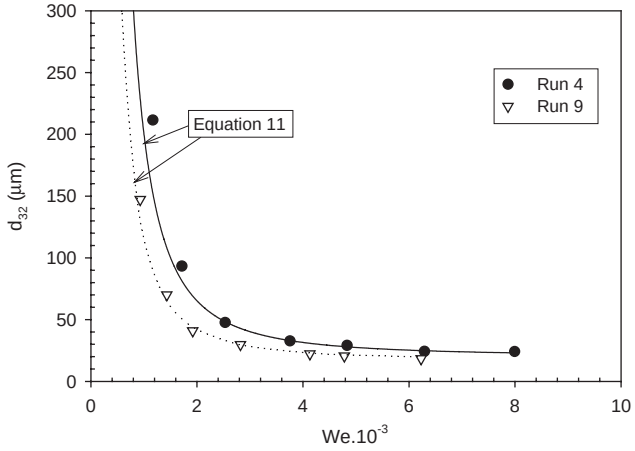

Fig. 5. Experimental data and drop size diameter model versus Weber number—runs 4 and 9.

that eliminate discontinuities in between different operating regimes, as in laminar, transitional and turbulent flow, by enlarging the range of Weber number. Therefore, the experimental data were used to obtain an equation for the effective interfacial area of this reacting system. The STATISTICA '99 Edition software package has been used in the non-linear regression study undertaken and Eq. (10) was the best obtained,

$$a = \frac{1}{\left[1 + \left(\frac{C_1}{We.\varepsilon}\right)^2\right](C_2\varepsilon^2 + C_3\varepsilon)}, \tag{10}$$

where C_1, C_2 and C_3 are adjustable constants referring to normalized operating variables and assume the values listed in Table 6 for each impeller type. Eq. (10) represents remarkably well this system without introducing other variables than the two mostly used to calculate the Sauter diameter: Weber number and hold-up fraction. Combining Eqs. (10) and (1), it is possible to calculate the drop-size diameter by Eq. (11):

$$d_{32} = 6\varepsilon\left[1 + \left(\frac{C_1}{We.\varepsilon}\right)^2\right](C_2\varepsilon^2 + C_3\varepsilon). \tag{11}$$

It is important to note that this study gives a contribution to the interfacial area and drop-size quantification in liquid–liquid systems in the lower Weber number operating range, which usually is not studied or was possible to quantify in previous studies. This can be confirmed in Fig. 5 where

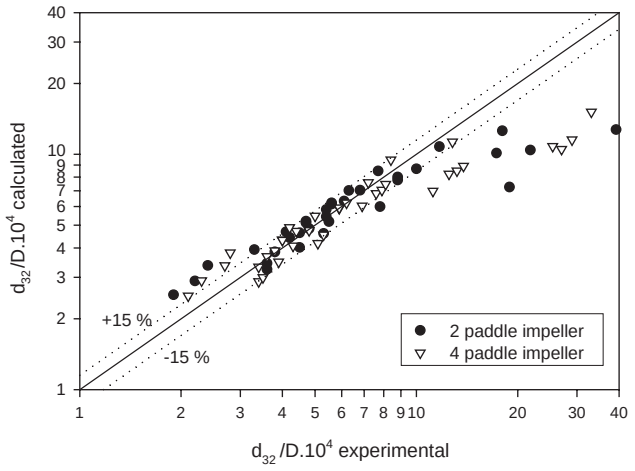

Fig. 6. Parity plot of d_{32}/D values calculated by Eqs. (8) and (9) and experimental.

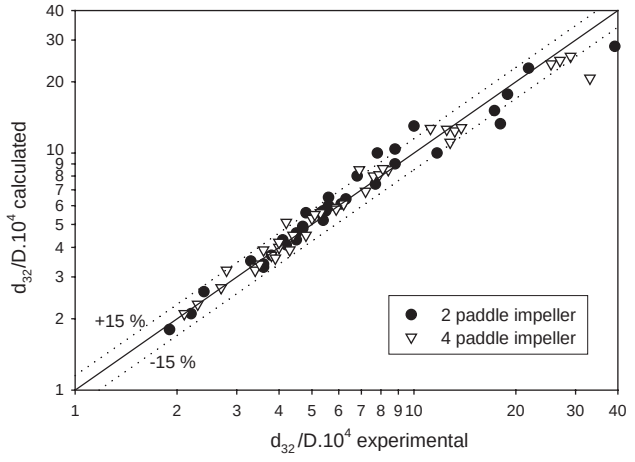

Fig. 7. Parity plot of d_{32}/D values calculated by Eq. (11) and experimental.

experimental data from runs 4 and 9 are plotted again, now over the all range of Weber number tested, and exhibit a good match with Eq. (11), even for low Weber number.

When a new model is proposed it is relevant to put it to the same test as previous models and this is achieved in Figs. 6 and 7, where parity plots of the experimental and calculated dimensionless Sauter mean diameters are represented. Eqs. (8) and (9), obtained in this study for a fixed −0.6 exponent on Weber number, have been used to build Fig. 6 over the entire range of experimental conditions tested. The striking feature in Fig. 6 is that restrictions have to be settled when using Eqs. (8) and (9), as referred to before in this work. These equations fail mainly for the bigger diameters, which correspond to lower Weber numbers, where turbulent flow regime is not well developed. The failure of Eq. (2) in fitting the drop size data with a constant exponent of −0.6 was already reported by other authors, namely by Fernandes and Sharma (1967) for lower stirring range and more recently by Desnoyer et al. (2003) that report the change of the Weber number exponent with the hold-up fraction for coalescent and non-coalescent systems. Desnoyer et al. (2003) reported that this exponent decreases in absolute value with the increase of the hold-up fraction, assuming −0.6 only when hold-up fraction tends to zero, which confirms restrictions to this equation that depend also on composition. The model proposed here in Eq. (11) is tested in Fig. 7. For $We > 1400$, using 29 experimental data, the relative average error of d_{32}/D is 8.1% for the two-paddle impeller and 5.9% for the four-paddle impeller when using 33 experimental data. When the whole range of Weber number tested is considered, average errors rise to 9.2 and 7.0% for the two- and four-paddle impellers, with 34 and 37 experimental data, respectively. Considering the uncertainty associated with experimental quantification of the process, these results are good. By comparing Figs. 6 and 7, one confirms that Eq. (11) improves the fitting over the entire range of agitation conditions tested in this liquid–liquid system, particularly for the lower and the higher d_{32}/D range. Taking into account that two different impellers have been tested and that even in industrial practice low Weber numbers can be present, the model proposed to calculate the Sauter mean drop diameter for these liquid–liquid dispersions is a significant contribution, particularly for the transitional flow regime.

In order to study the influence of the impeller diameter on the effective interfacial area, the diameter ratio between the impeller in use and the biggest impeller diameter used (in this case the two-paddle impeller) was introduced in Eq. (10). As a result, the constants C_2 and C_3 in Eq. (10) become independent of impeller diameter leading to Eq. (12) with C_1 listed in Table 6. Other tests with different impellers are required to fully support Eq. (12) and predict C_1.

$$a = \frac{D_{\text{ratio}}}{\left[1 + \left(\frac{C_1}{We.\varepsilon}\right)^2\right](-1.40\varepsilon^2 + 2.41\varepsilon)}. \tag{12}$$

In liquid–liquid agitated systems, it is usual to associate the decrease in drop size of the dispersed phase to an increase in effective interfacial area. However, this is only valid for particular hold-up fractions and this might lead to some misunderstanding of these processes. In Fig. 8, in order to distinguish each run, the drop size diameter axis was zoomed. In runs 1, 4 and 5 the hold-up fraction was varied and Fig. 8 illustrates that, for the same Weber number, d_{32} diminishes with the hold-up fraction decreasing. The corresponding interfacial areas are plotted in Fig. 9, where it is registered an intersection of curves for the higher *We* range, which does not occur for the drop size diameter. This pattern is registered in other runs and for the two stirrers studied, and can be easily understood taking into account that the interfacial area is inversely proportional to d_{32}, but directly proportional to the hold-up fraction. Therefore, when it is relevant to increase the interfacial area it is not straightforward that it will be achieved by increasing the hold-up fraction, since this result depends also on the ability to obtain a finely

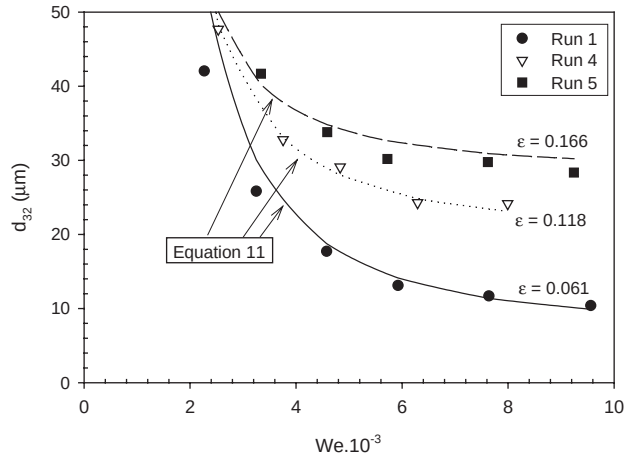

Fig. 8. Influence of hold-up fraction and Weber number on Sauter diameter—two paddle impeller.

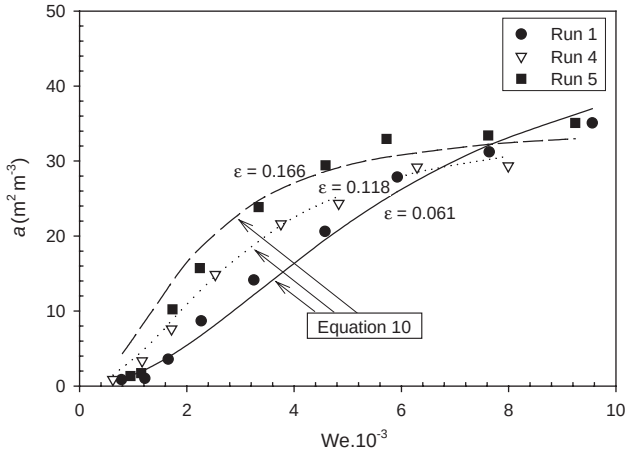

Fig. 9. Influence of hold-up fraction and Weber number on interfacial area—two paddle impeller.

dispersed phase of small droplets. In this case smaller hold-up fractions produce an efficient dispersion and allow achieving the same or even a larger effective interfacial area using less dispersed organic phase. In summary, it is possible to use a smaller hold-up fraction and achieve higher interfacial areas for the same *We* and stirring speed, as illustrated in Fig. 9. am Ende et al. (1995) also show the existence of a given volume acid percentage in alkylation dispersions that produces a maximum interfacial area in the reactor. Recently, Desnoyer et al. (2003) reported a non-linear behaviour of drop size with hold-up fraction, occurring a maximum of the Sauter mean diameter for intermediary hold-up fractions in coalescent dispersions systems.

The main conclusions of the work reported here are summarized in the three-dimensional plot in Fig. 10. Using normalized coordinates the experimental values for the two-paddle agitator are plotted as well as the surface represented by model Eq. (10). Confirming previous studies,

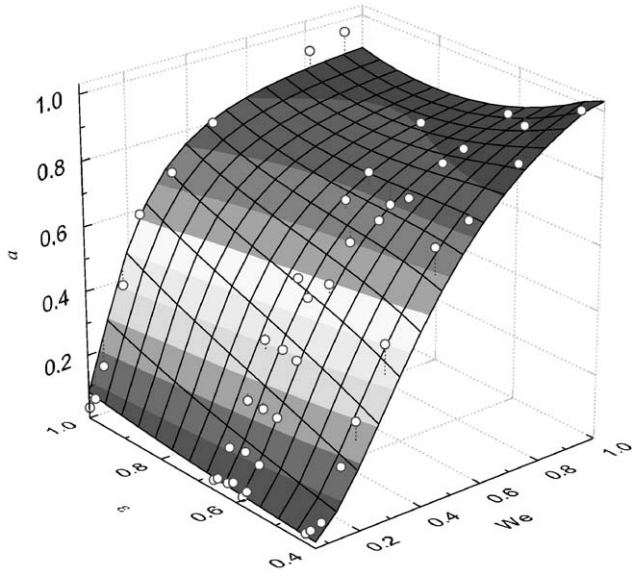

Fig. 10. Three-dimensional plot of effective interfacial area as function of hold-up fraction and Sauter mean drop diameter for the two paddle impeller.

the effective interfacial area increases with Weber number and stirring speed. Nevertheless, an increase in the fraction of dispersed phase is not always converted into a larger effective interfacial area. This is mainly true in the higher range of Weber number tested in this study where the surface in Fig. 10 shows a concavity.

5. Conclusions

A chemical method has been used to calculate the effective interfacial area of a liquid–liquid mixture in a baffled continuous stirred reactor. The chemical system used was diisobutylene diluted in benzene, the former extracted to the aqueous continuous phase to react with sulphuric acid. The specific mass transfer rate through the interface of this reacting system was measured in a batch-stirred cell of constant known interfacial area. At a second step, experiments were performed in a continuous reactor and the stirring speed, the hold-up fraction and the agitator have been changed.

The Sauter mean drop size diameter was correlated to the Weber number and the hold-up fraction using the equation in literature, which proved not to fit the wide range of experimental conditions tested, especially when lower stirring speed ranges were included. For the continuous stirred reactor and reacting system tested, a new empirical model was developed to predict the interfacial area and the Sauter mean drop diameter in a large range of stirring speed. This new equation allows matching experimental data and calculated values within a maximum relative average error of 9.2% for both impellers and the entire range of Weber number studied. No influence of residence time was registered in our experiments, as already reported by Godfrey et al. (1989).

In a liquid–liquid system, a good dispersion with small drops and high interfacial area can sometimes be obtained with a low hold-up fraction, as long as high stirring speed is used. This has been confirmed experimentally and contradicts expectations for interfacial area to continuously grow by increasing hold-up fraction of the dispersed phase.

The main limitation to the work reported here is that the tests only considered dispersions with hydrocarbon in acid-continuous phase at constant physical properties and temperature. A large number of experiments were conducted in the pilot plant operated continuously in a total of 90 steady states, which ensure a great consistency and credibility to the results reported here. Nevertheless, it should be stressed that this model is valid in this range of hold-up fractions, Weber numbers and for the impellers used, precautions being necessary in its extrapolation. It would be interesting to achieve a further validation of these results by a cross-check of the drop size information obtained by the chemical method with image analysis for the same reactor. This would allow registering the drop size distribution that would be compared to the Sauter diameter obtained by the chemical method.

Notation

a	effective interfacial area, $m^2\ m^{-3}$
A_{sc}	interfacial area of the stirred cell, m^2
$C_{i,j}$	molar concentration of compound i in the j phase, mol m^{-3}
d_{32}	Sauter mean drop diameter, m
D	impeller diameter, m
D_i	diffusion coefficient of component i, $m^2\ s^{-1}$
D_{ratio}	$\left(=\frac{D_{\text{impeller used}}}{D_{2\text{ paddle impeller}}}\right)$
F_A	molar flow of compound A in organic phase, mol s^{-1}
J_i	molar flux of component i, mol $m^{-2}\ s^{-1}$
k	pseudo-first-order kinetic constant, s^{-1}
m_i	distribution coefficient of component i
n	stirring speed, s^{-1}
N	stirring speed, rpm
t	time, s
V	reactor volume, m^3
V_i	volume of i phase, m^3
We	Weber number $\left(=\frac{n^2D^3\rho_c}{\sigma}\right)$

Greek letters

ε	hold-up fraction of dispersed phase
ρ_c	density of the continuous phase, kg m^{-3}
σ	interfacial tension, N m^{-1}
τ	residence time, min

Superscripts

i	interfacial
in	inlet stream of reactor
o	initial
out	outlet stream of reactor

Subscripts

aq	aqueous phase
B	benzene
DIB	diisobutylene
org	organic phase

Acknowledgements

The first author wishes to thank the Foundation for Science and Technology, Portugal, for his PhD Grant SFRH/BD/1266/2000. Both authors wish to thank the support provided by Quimigal, S.A. and acknowledge the assistance in the experimental work of Catarina Viana and Raquel Costa. We wish to dedicate this work to the memory of Prof. José Almiro e Castro.

References

Baldyga, J., Bourne, J. R., Pacek, A. W., Amanullah, A., & Nienow, A. W. (2001). Effects of agitation and scale-up on drop size in turbulent dispersions: Allowance for intermittency. *Chemical Engineering Science*, *56*, 3377–3385.

Balmelli, M., Steiner, L., & Hartland, S. (2000). Behaviour of turbulent dispersions in stirred single-stage cell. *Chemical Engineering Science*, *55*, 1653–1660.

Carey, F. A. (1992). *Organic chemistry* (2nd ed.). New-York: McGraw-Hill, inc.

Cieszkowski, J., & Dylag, M. (1994). Application of the sulfite method to the determination of the interfacial area in stirred-tank reactors. *International Chemical Engineering*, *34*(4), 511–517.

Coulaloglou, C. A., & Tavlarides, L. L. (1976). Drop size distributions and coalescence frequencies of liquid–liquid dispersions in flow vessels. *A.I.Ch.E. Journal*, *22*(2), 289–297.

Desnoyer, C., Masbernat, O., & Gourdon, C. (2003). Experimental study of drop size distributions at high phase ratio in liquid–liquid dispersions. *Chemical Engineering Science*, *58*, 1353–1363.

Eckert, R. E., McLaughlin, C. M., & Rushton, J. H. (1985). Liquid–liquid interfacial areas formed by turbine impellers in baffled, cylindrical mixing tanks. *A.I.Ch.E. Journal*, *31*(11), 1811–1820.

am Ende, D. J., Eckert, R. E., & Albright, L. F. (1995). Interfacial area of dispersions of sulfuric acid and hydrocarbons. *Industrial and Engineering Chemistry Research*, *34*, 4343–4350.

Fernandes, J. B., & Sharma, M. M. (1967). Effective interfacial area in agitated liquid–liquid contactors. *Chemical Engineering Science*, *22*, 1267–1282.

Gehlawat, J. L., & Sharma, M. M. (1968). Absorption of isobutylene in aqueous solutions of sulphuric acid. *Chemical Engineering Science*, *23*, 1173–1180.

Godfrey, J. C., Obi, F. I. N., & Reeve, R. N. (1989). Measuring drop size in continuous liquid–liquid mixers. *Chemical Engineering Progress*, *85*(12), 61–69.

Lasheras, J. C., Eastwood, C., Martínez-Bazán, C., & Montañés, J. L. (2002). A review of statistical models for the break-up of an immiscible fluid immersed into a fully developed turbulent flow. *International Journal of Multiphase Flow*, *28*, 247–278.

Nanda, A. K., & Sharma, M. M. (1966). Effective interfacial area in liquid–liquid extraction. *Chemical Engineering Science*, *21*, 707–714.

Podgórska, W., & Baldyga, J. (2001). Scale-up effects on the drop size distributions of liquid–liquid dispersions in agitated vessels. *Chemical Engineering Science*, *56*, 741–746.

Ribeiro, L. M., Regueiras, P. F. R., Guimarães, M. M. L., Madureira, C. M. N., & Cruz-Pinto, J. J. C. (1997). The dynamic behaviour of liquid–liquid agitated dispersions—II. Coupled hydrodynamics and mass transfer. *Computers & Chemical Engineering*, *21*(5), 543–558.

Sankholkar, D. S., & Sharma, M. M. (1973). A new system for the measurement of effective interfacial area in agitated liquid–liquid contactors by the chemical method. *Chemical Engineering Science*, *28*, 2089–2092.

Schiefferle, D.F., Hanson, C., & Albright, L.F. (1976). Heterogeneous nitration of benzene. In L. F. Albright, & C. Hanson (Eds.), *Industrial and laboratory nitrations*, (pp. 176–189). Washington: ACS Symposium Series.

Starks, C. M. (1999). Interfacial area generation in two-phase systems and its effect on kinetics of phase transfer catalyzed reactions. *Tetrahedron*, *55*, 6261–6274.

van-Woezik, B. A. A., & Westerterp, K. R. (2000). Measurement of interfacial areas with the chemical method for a system with alternating dispersed phases. *Chemical Engineering and Processing*, *39*(4), 299–314.

Vázquez, G., Cancela, M. A., Riverol, C., Alvarez, E., & Navaza, J. M. (2000). Determination of interfacial areas in a bubble column by different chemical methods. *Industrial and Engineering Chemistry Research*, *39*, 2541–2547.

Vermeulen, T., Williams, G. M., & Langlois, G. E. (1955). Interfacial area in liquid–liquid and gas–liquid agitation. *Chemical Engineering Progress*, *51*(2), 85–94.

Westerterp, K. R., Van Dierendonck, L. L., & De Kraa, J. A. (1963). Interfacial areas in agitated gas–liquid contactors. *Chemical Engineering Science*, *18*, 157–176.

Zaldivar, J. M., Molga, E., Alós, M. A., Hernandez, H., & Westerterp, K. R. (1996). Aromatic nitrations by mixed acid. Fast liquid–liquid reactions regime. *Chemical Engineering and Processing*, *35*(2), 91–105.